CORROSION BEHAVIOR IN AQUEOUS ENVIRONMENTS OF MARTENSITIC STAINLESS STEELS USED IN HYDROPOWER TURBINE BLADES

George COMAN[1], Andrei BERBECARU[1*], Marian Nicolae COSTEA[1], Mirela SOHACIU[1], Ecaterina MATEI[1], Andra PREDESCU[1], Sorin CIUCA[1], Cristian PREDESCU[1]

The paper presents the results of research carried out on three samples of martensitic stainless steel used in the manufacture of hydropower turbine blades. The experiments were carried out under normal aeration conditions at ambient temperature (22 degrees C) in freshly prepared solutions of 1N potassium sulfate and 3% NaCl. The corrosion rates were calculated using the Tafel slope method.

Analysis of the results regarding the corrosion behavior in Cl-free environments coupled with the microstructural information obtained by SEM highlights very good corrosion resistance properties (very good resistance class) as well as the appropriate passivation of the surface. This recommends the three steels for use in the construction of hydropower turbine blades. The negative influence of chlorine on the surface is highlighted by reducing the degree of passivation by half, which does not recommend the use of this material in a saline environment.

Keywords: martensitic steel, corrosion, hydro, blades, passivation.

1. Introduction

One of the main sources of renewable energy that is currently used worldwide is that produced in hydroelectric plants. Although they involve high investment costs, they present the advantage of using water, a practically inexhaustible resource. The current technology has allowed the functional optimization of the turbines, with mechanical yields and high performances, the main problems remaining to be solved being related to their maintenance.

In a hydropower plant, the component parts of the turbines have the greatest exposure to damage, the factors leading to this result being related to the path and quality of the water, the kinematics and dynamics of the turbine and the operating regime. The main causes contributing to increased downtime for

[1] *Corresponding author
Faculty of Materials Science and Engineering, UNSTPB, Bucharest, Romania, e-mail: andrei.berbecaru@upb.ro

repairs are cracking and erosion of the rotor and vanes. These are generally generated by material or manufacturing defects, fatigue or overloads.

The erosion is caused by the sand drawn into the turbine together with the water as well as by the phenomenon of hydrodynamic cavitation (cavitational erosion). Cavitational erosion craters often have depths of the order of millimeters. Thus, the affected areas are sometimes perforated in the case of hydraulic turbine rotor blades, the most affected by cavitational erosion. In the case of stainless steels, specialized literature indicates 3 types of corrosion: intercrystalline, cavitation and pitting.

Frankel et al. [1] provided as critical factors the effect of the composition of the alloy, the value of the potential and the temperature at which corrosion occurs. The possible factors involved in corrosion are shown in Fig. 1. These factors are: (1) physical factors (2) chemical factors (3) biological factors and (4) metallurgical factors. The factors that can affect pitting in Fig. 1 are composed of all types of exposure areas. The influencing factors are not limited to the case of stainless steels, light and low-alloy steels are also taken into account, the specialized literature indicating similar corrosion behavior [2]; [3]; [4].

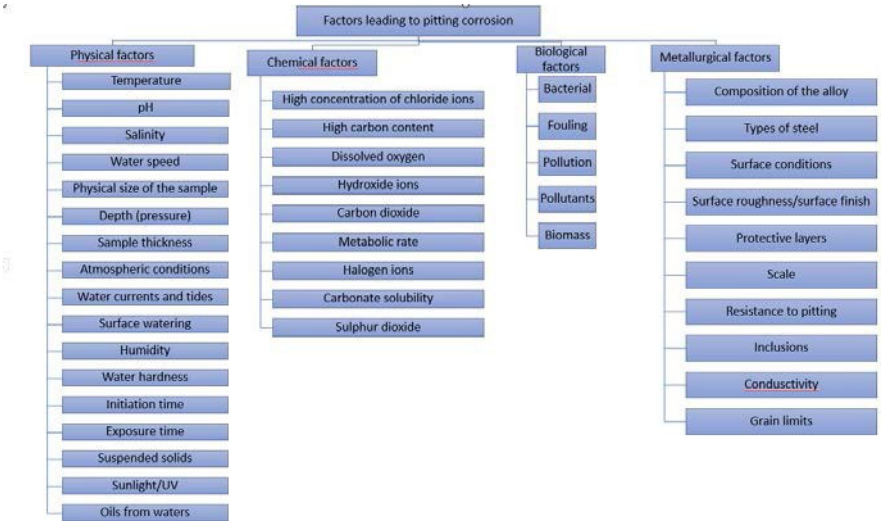

Fig. 1. Factors that can affect pitting corrosion [3]

When the cavitation fluid is corrosive, the loss of material is not purely mechanical in nature, as corrosion occurs. When cavitation occurs in a corrosive environment, erosion-induced corrosion and/or corrosion-induced erosion will intensify the damage process and can be called “erosion-corrosion cavitation” [5, 6]. Erosion and corrosion often occur synergistically and material loss can be significantly greater than the sum of the effects of the processes acting separately

[11]. An example is the difference between erosion-corrosion (EC) rates in distilled water and 3.5% NaCl solution [6]. In addition to the impact of corrosion on EC, it can be accelerated by the synergistic effect due to erosive wear. Also, if the cavitation fluid contains erosive particles, then the bursting bubbles entrain the particles hitting the surface at high speed. The rate of erosion is higher than the rate of corrosion or erosion caused by solid particles as a singular phenomenon in the case of hydraulic turbines operating in sandy water [7, 8]. To mitigate EC, three approaches can be addressed concurrently: improving design to minimize large hydrodynamic pressure differences; changing environmental conditions, eg temperature and fluid corrosiveness; selecting more resistant materials or applying a protective layer against EC. Unfortunately, changing designs and controlling environmental conditions are not easy options when the third approach is the most feasible. In general, selection criteria for EC-resistant materials include hardness, martensitic transformability, (lowstacking defect energy) for cavitation energy absorption, and corrosion resistance. [9] [14].

The phenomenon of erosion by corrosion is a subject that covers all aspects of their mainly mechanically induced interactions with electrochemical processes. The diagram in fig. 2 illustrates the processes that occur during the interaction between fluids with various flow rates and the material.[13]

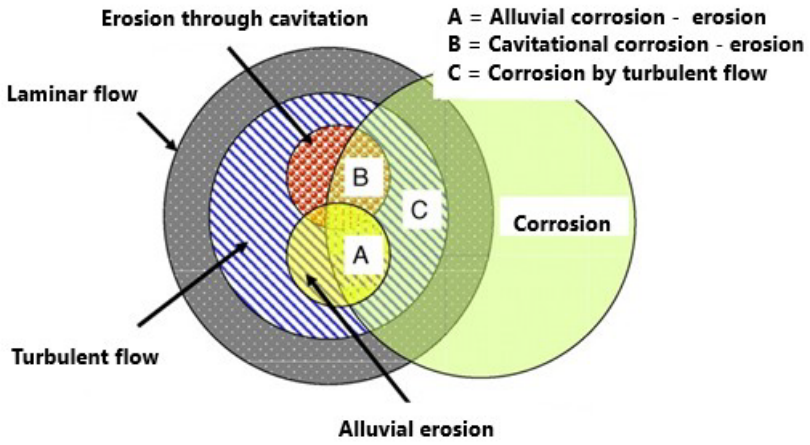

Fig. 2 Representation of possible erosion-corrosion interactive zones at different flow rates: (A) corrosion - alluvial erosion, (B) corrosion-erosion by cavitation and (C) corrosion by turbulent flow [9]

2. Materials and Methods

To carry out the research, 3 stainless steels were developed for which a cold crucible furnace was used, in vacuum and argon atmosphere, of the Fives Celes ALU 600 type.

The calculation of the furnace load considered obtaining a composition of the stainless steels positioned in the Schaeffler diagram in the areas marked in fig. 3.

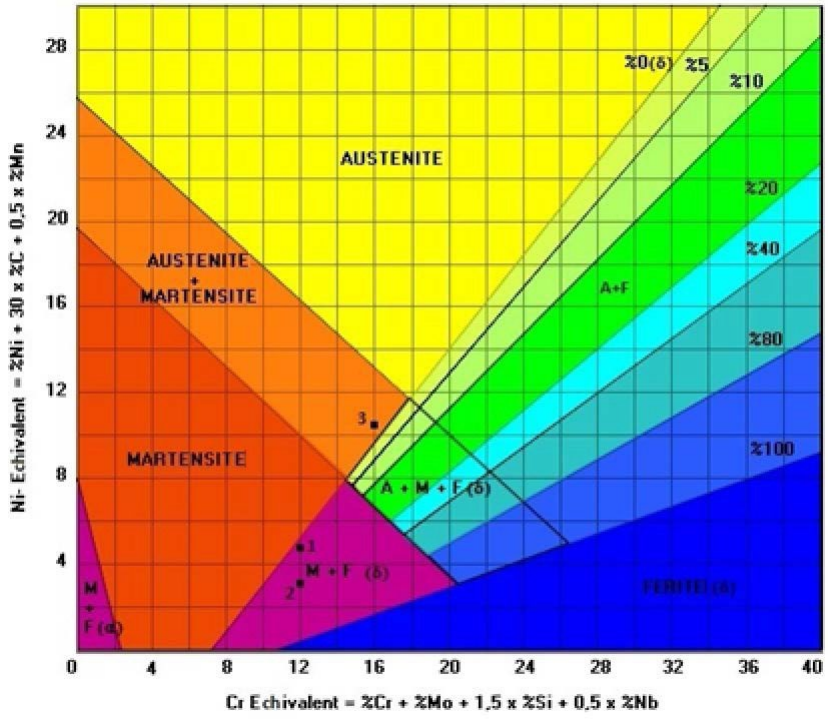

Fig. 3 Positioning in the Schaeffler diagram of the steels developed for research experiment

The chemical composition of the developed steels is presented in table 1.

Three batches were developed, P1, P2, P3, with the following compositions:

Table 1:

	Cr	Ni	Mo	Si	Cu	Mn	Ti	Al	Nb	C	V	Co	P	S	Fe
P1	11.78	4.34	0.002	0.182	0.078	0.550	0.001	0.0061	0.012	0.042	0.025	0.016	0.0079	0.0085	82.95
P2	12.05	3.85	1.024	0.393	0.170	0.676	0	0.0282	0.0438	0.0426	0.0081	0.0299	0.0287	0.0114	81.64
P3	9.92	9.61	5.07	0.295	0.147	0.351	0.923	0.049	0.0889	0.0223	0.0022	0.0356	0.0204	0.0204	73.8

The determination of the chemical composition of the stainless steels

developed for the experiments was carried out with the optical emission spectrometer Leco GDS 500 A. For the metallographic etching, the Marble reagent was used for 45 seconds. The Quanta 450 FEG electron microscope was used for the scanning electron microscopy (SEM) and energy dispersive X-ray spectroscopy (EDX) analysis. A Gamry Reference 600 potentiostat/galvanostat was used to analyze the corrosion behavior with the specialized software for analyzing the acquired data Echem Ana-lisys. The electrochemical cell was a classic one with three electrodes, the working electrode (the sample), the platinum counter electrode and the reference electrode (the calomel saturated electrode).[12] The technique used was the anodic polarization of the electrode in the range -250 mV - +1000 mV to characterize the passivation capacity of the electrode, and to determine the corrosion rates, the Tafel slope method was used with polarization between - 250 mV - +250 mV around stationary potential with a potential scanning speed of 1mV/s in freshly prepared solutions of 1N potassium sulfate and 3% NaCl.

3. Results

The polarization curves for aqueous medium without chlorine (which is the working medium of hydro turbines) are shown in fig. 4 and the polarization curves for aqueous medium with chlorine are shown in fig. 4.

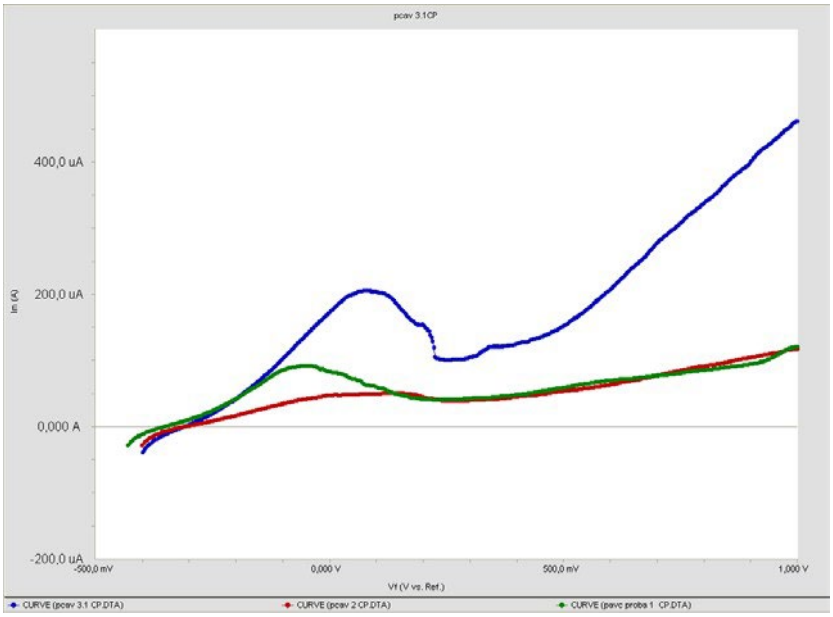

Fig. 4 Anodic polarization curves of the three samples in 1N Na2SO4 solution at room temperature with a polarization rate of 1mV/s

From the analysis of the anodic polarization curves presented in fig. 4, the following aspects emerge: all the steels show the tendency of passivation in an aqueous environment free of chlorine, specifying that steel 3 shows a more pronounced anodic domain considering the chromium content below the 12% limit theoretical for a stainless steel. However, the general corrosion behavior of this material is compensated by the approx. 10% Ni content, which leads the structure to the mostly martensitic range. Although we cannot speak of an actual passivation of the surface, it must be stated that the current density values are around uA/cm2 for all materials, including in the field of active dissolution. Fig. 5 and table 2 present the results of the Tafel analysis. [15]

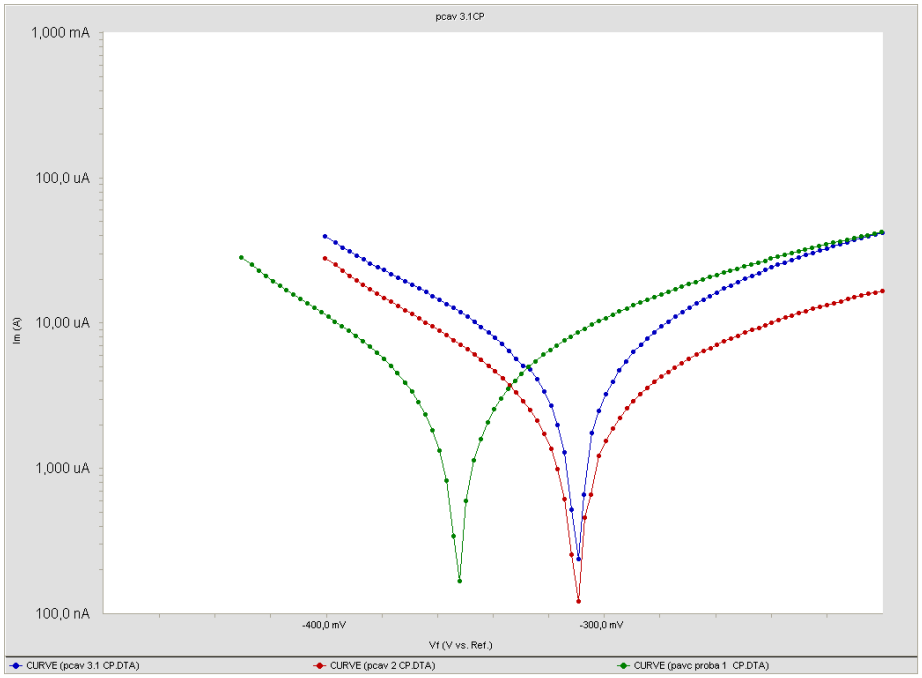

Fig. 5 Tafel curves of the 3 samples in 1N sodium sulfate

Table 2

Calculation results

	Beta A* V/decade	Beta C* V/decade	Icorr* uA	Ecorr* mV	Corr rate* mpy
1	256,2 e-3 V/decade	199,6e-3 V/decade	10,4 uA/cm2	-353,0 mV	5,127 mpy
2	177,7e-3 V/decade	125,6e-3 V/decade	4,63 uA/cm2	-310,0 mV	2,03 mpy
3	131,4e-3 V/decade	141,5e-3 V/decade	8,32 uA/cm2	-310,0 mV	3,654 mpy

*Beta A slope of the anodic line, Beta C slope of the cathodic line, Icorr corrosion current density, Ecorr corrosion potential, Corr rate corrosion rate

From Fig. 5 it can be seen that samples 2 and 3 have practically the same value of the corrosion potential located approximately 50mV more electropositive, which indicates an increased tendency of passivation. The corrosion rate of 3.654 mpy (0.0928 mm/year) places the material according to the standard in the corrosion resistant class. From this point of view, all 3 materials fall into the same resistance class, the differences in corrosion speed being of the order of 1.5 mpy. The SEM analysis of the samples subjected to corrosion did not show any change in the surface, as can be seen in fig. 6.

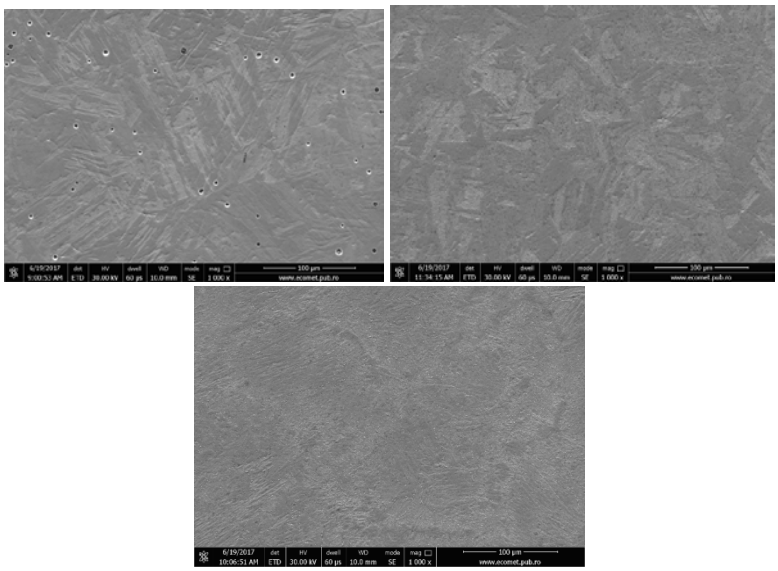

Fig. 6 SEM images of the 3 samples after corrosion in environment without Cl

Considering the fact that there are no significant differences between the 3 materials in terms of their corrosion behavior, they were subjected to much harsher conditions, namely in a 3% sodium chloride solution (in a first approximation, simulated sea water). The analysis of the behavior of the materials in NaCl3% solution is presented in fig. 7-8 and table 3.

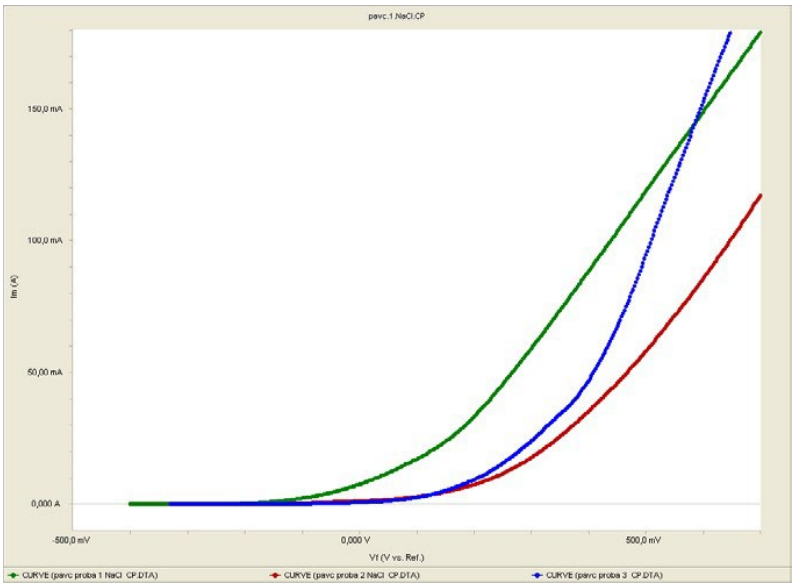

Fig. 7 Anodic polarization curves of the three samples in 1N NaCl solution at room temperature with a polarization rate of 1mV/s

The increased aggressiveness of the test environment, i.e. the high amount of chlorine ions prevents the passivation of the surfaces, practically the corrosion current increases continuously reaching relatively high values of the order of mA/cm2 and the polarization curves suddenly change the Di/Du slope to much more electronegative values of comparative potential with the previous medium (sulfate), and the current densities are of the order of mA/cm2. Between steels 2 and 3 the differences are insignificant. The polarization curves practically overlap over a relatively wide range of potential.

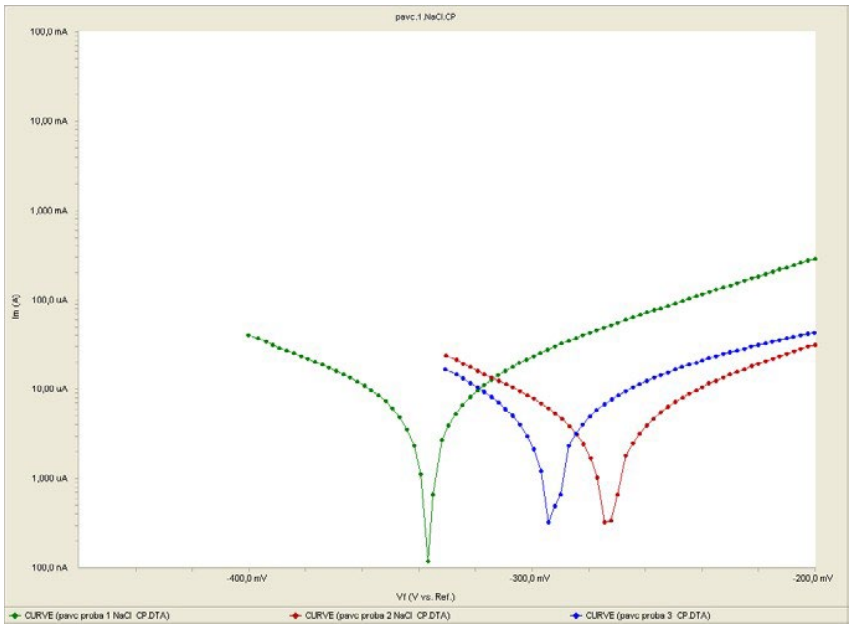

Fig. 8 Tafel curves of the 3 samples in 3% NaCl solution

Table 3

Calculation results

	Beta A* V/decade	Beta C* V/decade	Icorr* uA	Ecorr* mV	Corr rate* mpy
1	93.7e-3	113e-3	11	-337,0	5.417
2	94.9e-3	91,9e-3	5.63	-273,0	2.766
3	106,7e-3	85,e-3	7	-293,0	3.443

* Beta A slope of the anodic line, Beta C slope of the cathodic line, Icorr corrosion current density, Ecorr corrosion potential, Corr rate corrosion rate

Regarding the corrosion speed values, all the samples fall in accordance with the norms in the "very resistant - resistant" resistance classes, stating that in environments with chlorine, the general corrosion speed is not an indicator of the corrosion resistance performance due to the triggering local depassivation processes (corrosion points).

Fig. 9 Macro image of the three samples after the electrochemical corrosion test

Samples 1 and 2 showed large attacks of the order of millimeters that seem to follow a preferential direction on the surface. When analyzing in detail by SEM microscopy of sample 1, it was observed that the attack started at the interface of the ferrite particles with the areas resulting from the decomposition of martensite and continued by the dislocation of large surfaces of the material advancing into intercrystalline material, fig. 10.

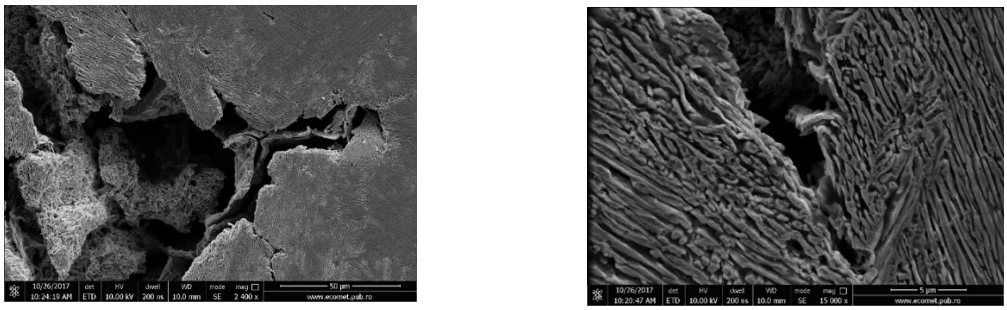

Fig. 10 SEM images of the surface appearance of sample 1 at magnification x2400 and x15000

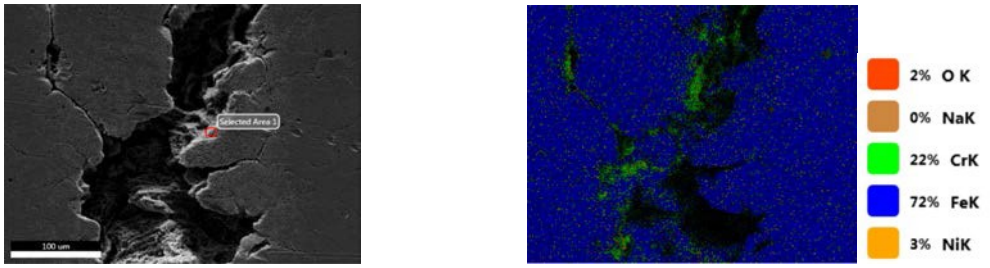

Fig. 11 The distribution of the homogeneity of the elements on the analyzed area from sample 1

Sample 2 presented the same type of surface attack with material dislocations but without a selective attack of phases being detected at the micro level, fig. 12.

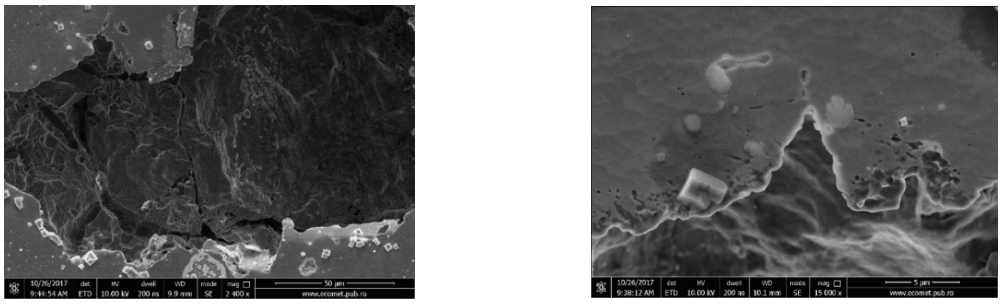

Fig. 12 SEM images of the surface appearance of sample 2 at magnifications of x2400 and x15000

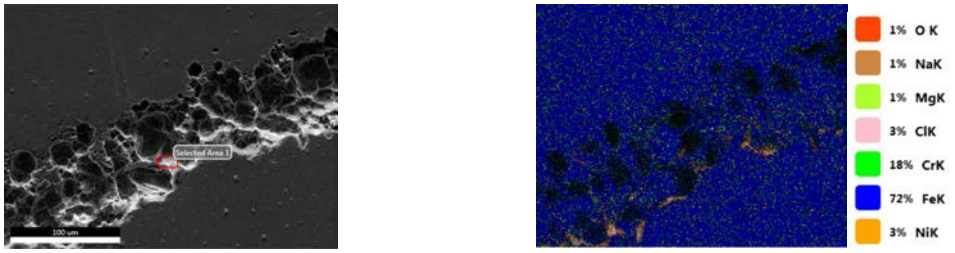

Fig. 13 The distribution of the homogenity of the elements on the analyzed area from sample 2

Increasing the content of Cr, Ni and Mo significantly increases the resistance to corrosion in the presence of Cl ions, so the surface of sample 3, from a macroscopic point of view, is the least affected, showing localized attacks of very small sizes. SEM analysis did not highlight selective attacks of phases, structure not being affected, fig. 14.

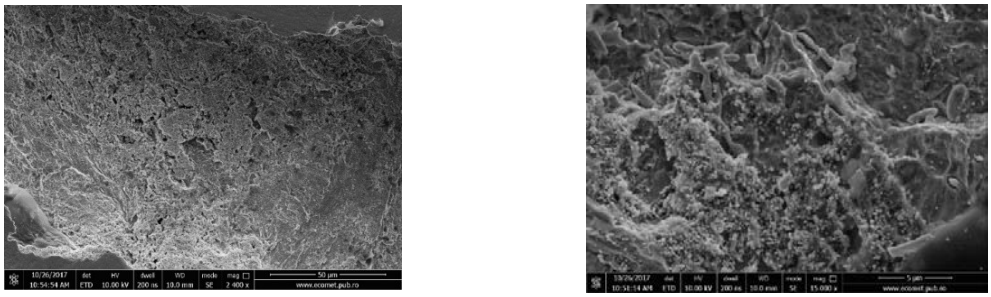

Fig. 14 SEM images of the surface appearance of sample 3 at x2400 and x15000 magnifications

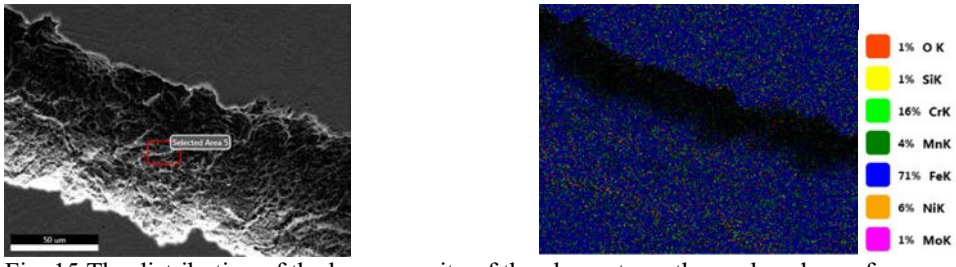

Fig. 15 The distribution of the homogeneity of the elements on the analyzed area from sample 3

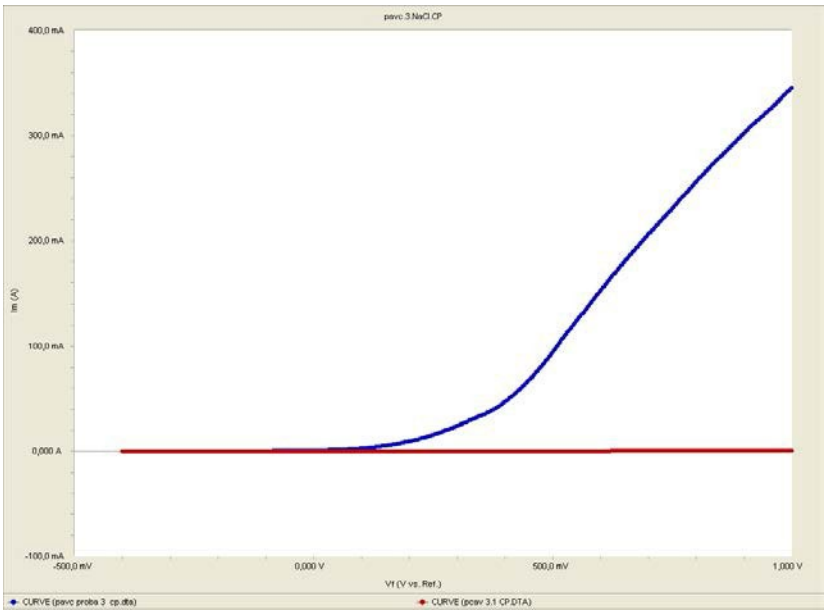

Fig. 16 Polarization curves obtained on steel 3 in the presence (blue curve) and absence (red curve) of chlorine

The very good corrosion behavior of steel 3 in chlorine-free environments is highlighted by comparing the polarization curves obtained on this material in the presence and absence of chlorine, fig. 16.

Analysis of all the results regarding the corrosion behavior in Cl-free environments of alloy 3 coupled with the microstructural information obtained by SEM highlights very good corrosion resistance properties (very good resistance class) as well as the appropriate passivation of the surface. This recommends it for use in the construction of hydro turbine vanes.

It is evident the negative influence of chlorine on the surface by reducing the area of passivity by half, which does not recommend the use of this material in a saline environment.

4. Conclusions

After electrochemical corrosion testing, it was found that samples 1 and 2 showed millimeter-sized attacks that appear to follow a preferential direction on the surface. When analyzing in detail by SEM microscopy of sample 1, it was observed that the attack started at the interface of the ferrite particles with the areas resulting from the decomposition of martensite and continued by the dislocation of large areas of the material advancing into the intercrystalline material.

Sample 2 presented the same type of surface attack with material dislocations, but without a selective phase attack being observed at the micro level.

From the analysis of the anodic polarization curves, the following aspects emerge: all the samples show the tendency of passivation in an aqueous medium free of chlorine, the general corrosion behavior of this material is compensated by the approx. 10% Ni content, which leads the structure to the mostly martensitic range.

Corrosion rates for all samples fall according to the norms in resistance classes very resistant - resistant, stating that in chlorine environments the general corrosion rate is not an indicator of corrosion resistance performance due to the triggering of local depassivation processes (points of corrosion).

The increase in the content of Cr, Ni and Mo significantly increases the corrosion resistance in the presence of Cl ions, thus the surface of steel 3, from a macroscopic point of view, is the least affected, showing localized attacks of very small sizes. The SEM analysis did not reveal selective phase attacks, the structure not being affected.

Following the electrochemical corrosion testing, it was found that samples 1 and 2 showed attacks of large dimensions of the order of millimeters that seem to follow a preferential direction on the surface.

Acknowledgements

This work was supported by a grant from the National Program for Research of the National Association of Technical Universities-GNAC ARUT 2023

R E F E R E N C E S

[1] *Frankel, G*., 1998. Pitting corrosion of metals a review of the critical factors. J. Electrochem. Soc. 145, 2186-2198.

[2] *Melchers, R.E*., 1994. Pitting Corrosion in Marine Environments: a Review. Department of Civil Engineering and Surveying, University of Newcastle.

[3] *Melchers, R*., 2004 a. Pitting corrosion of mild steel in marine immersion environment - part 2: variability of maximum pit depth. Corrosion 60, 937-944.

[4] *Melchers, R., Ahammed, M.,* 1994. Nonlinear Modelling of Corrosion of Steel in Marine Environments. Department of Civil Engineering and Surveying, University of Newcastle.

[5] *ASTM G119-09*, Standard Guide for Determining Synergism between Wear and Corrosion, ASTM, 2009.

[6] *C.T. Kwok, F.T. Cheng, H.C. Man,* Mater. Sci. Eng. A290 (2000) 145–154.

[7] *H. Jin, F. Zheng, S. Li, C. Hang*, Wear 112 (1986) 199–205.

[8] *H.J. Amarendra, G.P. Chaudhari, S.K. Nath*, Wear 290–291 (2012) 25–31.

[9] *C.T. Kwok, H.C. Manc, F.T. Chengc, K.H. Lo,* Surface & Coatings Technology 291 (2016) 189–204

[10] *Berbecaru, AC; Coman, G; Ciuca, S; Grecu, A; Gherghescu, IA; Dobre, M; Sohaciu, M; Matei, E; Predescu, AM; Diaconu, IA; Predescu, C*, Characterization of some rhenium inconel superalloys made in a vacuum induction furnace and cast in argon atmosphere, University Politehnica of Bucharest Scientific Bulletin Series B-Chemistry and Materials Science, Volume 86, Issue 2, Page 245-256

[11] *Grecu, A; Berbecaru, AC ; Coman, G ; Ciuca, S ; Matei, E ; Sohaciu, MG ; Gherghescu, IA ; Predescu, AM ; Predescu, C*, Assessment of premature degradation of a gas injection pipeline due to hydrogen released by the benzene hydrofining equipment, University Politehnica of Bucharest Scientific Bulletin Series B-Chemistry and Materials Science, Volume 85, Issue 2, Page 257-274

[12] *Gradinaru, CS; Coman, G; Ciuca, S; Sohaciu, MG; Berbecaru, AC; Grecu, A; Dumitrescu, RE; Gherghescu, IA; Predescu, C*, Research on corrosion degradation process of some thermal power plants steam boiler pipes, University Politehnica of Bucharest Scientific Bulletin Series B-Chemistry and Materials Science, Volume 83, Issue 3, Page 231-244

[13] *Coman, G., Ciuca, S., Berbecaru, A.C., Pantilimon, M.C., Sohaciu, M.G., Gradinaru, C., Predescu, C.,* New martensitic stainless steel hardenable by precipitation for hydropower turbines, în UPB Scientific Bulletin, Series B: Chemistry and Materials Science, Vol: 79, Issue 4, 2017, (pag. 209-218)